et al. [13] reported that ERα in osteocytes regulates trabecular bone formation and thus trabecular bone volume in male mice. These results are in contrast to our own findings showing that the precise molecular functions and target genes of ERα in osteocytes still remain elusive.

Osteocytes are embedded in the extracellular matrix of bone and represents more than 90% of the cells existing in bone. Osteocytes possess dendrites that extend throughout the bone and are used to communicate with each other and also with osteoblasts and osteoclasts on the surface of the bone. The function of osteocytes as mechanosensory cells is inferred from their shape and location [16]. In fact, mechanical loading and unloading change osteocyte gene expression in vivo, indicating that osteocyte function is affected by loading conditions [17–20]. In addition, they are known to be involved in mineral metabolism through expression of proteins such as FGF23, Phex, Mepe, and Dmp1 [21–24] (for review, see [25]). Recently, it has been postulated that osteocytes can orchestrate skeletal homeostasis through mineral metabolism as well as the regulation of osteoblastic bone formation and osteoclastic bone resorption by secretory proteins such as sclerostin and FGF23. Osteocytes are also reported to regulate osteoblastic bone formation through IGF-1, TGFβ, NO, PGE_2 and sclerostin and to regulate osteoclastic bone resorption through TGFβ, NO, and PGE_2, and RANKL/OPG [26].

Bone mass can be maintained by mechanical loading while unloading or immobilization decreases bone mass. In vivo unloading rodent models such as tail suspension can induce bone loss in hind limbs [27] and mechanical loading can increase bone mass in forelimbs [28]. The regulation of bone mass by mechanical loading is mediated, at least in part, through β-catenin signaling [29–31], and estrogen/ER signaling might also be involved in this mechanism [32].

In this study, we examined the functions of ERα in osteocytes by generating mice lacking ERα in osteocytes and analyzing osteocyte gene expression profiles and subjecting them to hindlimb unloading.

Materials and methods

Animals

The ERα floxed mutant ($ERα^{L2/L2}$) mice kindly provided by Dr. Chambon and null alleles with a C57BL/6 J background have been previously described [5]. $ERα^{L2/L2}$ mice were crossed with $Dmp1^{Cre}$ mice [33] to generate $Dmp1^{Cre}$; $ERα^{L2/+}$ mice, and $Dmp1^{Cre}$; $ERα^{L2/L2}$ ($ERα^{ΔOcy/ΔOcy}$) and $ERα^{L2/L2}$ ($ERα^{flox/flox}$) were obtained by crossing $Dmp1^{Cre}$; $ERα^{L2/+}$ and $ERα^{L2/L2}$. $Dmp1$-GFP mice were kindly provided by Dr. Ivo Kalajzic [34]. All mice were housed in a specific-pathogen-free facility under climate-controlled conditions with a 12-hour light/dark cycle and were provided with water and standard diet (CE-2, CLEA, Japan) ad libitum. All animals were maintained and examined according to the protocol approved by the Animal Care and Use Committee of the University of Tokyo.

Genome DNA extraction and cell culture

Various tissues (0.5 g) from $ERα^{ΔOcy/ΔOcy}$ were harvested, washed with PBS and lysed in 2 ml of lysis buffer with proteinase K (150 µg/ml) overnight. Also, DNA of osteocytes was isolated from the calvariae of $ERα^{ΔOcy/ΔOcy}$ in which cells on the surface of the bone such as osteoclasts and osteoblasts were removed by sequential enzymatic treatment. Primary osteoblasts obtained from the neonatal calvariae were cultured in αMEM (Life Technologies) containing 10% FBS (Cell Culture Bioscience), 50 µg/ml ascorbic acid (Sigma-Aldrich) and 10 nM β-glycerophosphate (Sigma-Aldrich) for 21 days. Cells were cultured with phenol red free media 24 h before cells were treated with 17β-estradiol. Primary osteoclasts were differentiated from the bone marrow obtained from 6-week-old $ERα^{ΔOcy/ΔOcy}$ mice using 10 ng/ml of M-CSF (R&D Systems) and 234 ng/ml of GST-RANKL (Oriental Yeast) for 5 days. The genomic DNA was extracted using phenol/chloroform and isopropanol precipitation.

ELISAs

Enzyme-linked Immunoassays, ELISAs, were was performed following the protocols of the Estradiol EIA Kit (Cayman Chemical Company) for estradiol, Testosterone EIA Kit (Cayman Chemical Company) for testosterone, and Rodent Luteinizing Hormone (LH) ELISA TEST (Endocrine Technologies) for LH.

Bone analyses

The BMD of femurs and tibiae obtained from 12-week-old littermates were measured by DXA using a bone mineral analyzer (DCS-600EX: ALOKA). Micro Computed Tomography scanning of the tibiae and femurs was performed using a Scanco Medical µCT35 System (SCANCO Medical) with an isotropic voxel size of 6 µm for trabecular analyses and 12 µm for cortical analyses according to the manufacturer's instructions and the recent guidelines of the American Society for Bone and Mineral Research (ASBMR) [35]. For bone histomorphometry, the mice were double-labeled with intra-peritoneal injections of 16 mg/kg of calcein (Sigma) at 5 and 2 days before sacrifice. Lumbar vertebral bodies were removed from each mouse and fixed with 4% PFA in PBS overnight. Lumbar vertebrae were embedded with MMA after dehydration and the plastic sections were cut by a standard microtome (LEICA) into 7 µm for von Kossa staining and 4 µm for TRAP and Toluidine-blue staining. The region of interest was the secondary spongiosa of L3 and L4. Sections were used for analyses when the bases of the bilateral transverse processes were opened. The region of interest (ROI) in the lumbar vertebral body is the secondary spongiosa, which is separated from the primary spongiosa, cranial and caudal growth plate, according to the same protocol as previously performed [8,36]. Histomorphometric analyses were performed using OsteoMeasure (OsteoMetrics, Inc., GA, USA) according to the ASBMR guideline [37].

Isolation of Dmp1-GFP positive osteocytes by FACS

A highly purified population of osteocytes was isolated from neonatal calvariae by FACS using a modified version of the protocol of Paic F et al. [38]. Cells were isolated from 10-day-old fetal mice calvariae of $ERα^{ΔOcy/ΔOcy}$ and $ERα^{flox/flox}$ also expressing Dmp1-GFP. After removal of the sutures, pooled calvarial tissue was subjected to six sequential, 30-minute digestions in a mixture containing 0.05%/0.2 mM trypsin/EDTA and 1.5 U/ml collagenase-P (Roche) at 37 °C. Cell fractions 4 to 6 were collected, pooled, and re-suspended in Dulbecco's modified Eagle's medium (DMEM, Life Technologies) containing 10% FBS (Hyclone) and centrifuged. Cells were rinsed with PBS and re-suspended in PBS/2% FBS and filtered through a 70-µm filter. Cell sorting was performed using a BD FACS Aria cell sorter. The gate for collecting GFP + cells was set as GFP + population to represent 10% to 15% of the total cells in GFP + mice and 0.8% to 1.0% of total cells in GFP − mice (negative control). GFP + cells were collected in a tube with 500 µl of PBS/3% FBS.

Gene expression microarray

Gene expression microarray was generated using total RNA extracted from the isolated GFP + osteocytes of $ERα^{ΔOcy/ΔOcy}$ and $ERα^{flox/flox}$ as previously described [8] and RNA samples were evaluated using the Affymetrix Mouse Genome 430 2.0 Array following standard Affymetrix protocols (GEO: GSE41997). Gene ontology analyses were performed using DAVID Bioinformatics Resources 6.7 [39].

RNA extraction and RT-qPCR

Total RNA from the pulverized femurs or sorted cells was extracted using TRIZOL (Invitrogen) and RNeasy purification kit (QIAGEN). First-strand cDNA was synthesized from total RNA using PrimeScript RT Master Mix (TaKaRa) and subjected to RT-qPCR using SYBR Premix Ex Taq II

(TaKaRa) or KAPA SYBR Fast qPCR Kits (KAPA Biosystems) with Thermal Cycler Dice (TaKaRa) according to the manufacturer's instructions. Primers were purchased from Takara Bio Inc. (Otsu, Japan) or Operon Biotechnologies (Tokyo, Japan) [8]. Gene expression levels were normalized by *Gapdh* or *Rplp0*. Primer sequences were as follow; *Rplp0*: F 5′-TTCCAGGCTTTGGGCATCA-3′ and R 5′-ATGTTCAGCATGTTCAGCAG TGTG-3′, *Gapdh*: F 5′-AAATGGTGAAGGTCGGTGTG-3′ and R 5′-TGAA GGGGTCGTTGATGG-3′, *ERα*: F 5′-CATGGTCATGGTAAGTGGCA-3′ and R 5′-TCTCTGGGCGACATTCTTCT-3′, *Dmp1*: F 5′-TGAAGAGAGGACGGGT GATT-3′ and R 5′-TCCGTGTGGTCACTATTTGC-3′, *Kera*: F 5′-TGGGATGT CCACGACGACTT-3′ and R 5′-AAGGCAGTAGGGAAACTGGGA-3′, *Mdk*: F 5′-TGGAGCCGACTGCAAATACAA-3′ and R 5′-GGCTTAGTCACGCGGA TGG-3′, *Sostdc1*: F 5′-AAATGTATTTGGTGGACCGC-3′ and R 5′-GAATCA AGCCAGGAATGGAG-3′.

Tail suspension

Tail suspension experiments were performed for female *ERα*$^{\Delta Ocy/\Delta Ocy}$ and *ERα*$^{flox/flox}$ mice for 4 weeks starting at 8 weeks of age according to previous reports [40,41]. Briefly, a stainless steel harness was superglued to the sides of the tail. Female *ERα*$^{\Delta Ocy/\Delta Ocy}$ and *ERα*$^{flox/flox}$ mice were then suspended from an eye bolt which was secured into the bars of the top of the rat cage. The animal could rotate 360° with the fish swivel and could also move backwards and forwards about 7.5 cm. Water was provided through a standard water bottle with an extra long angled sipper tube to allow the animals to reach the water. Control female *ERα*$^{\Delta Ocy/\Delta Ocy}$ and *ERα*$^{flox/flox}$ mice were chained to the cage top during the same period of time, but were allowed to load their hindlimbs to minimize the difference in stress-related effects between the tail-suspended groups and the control groups (n = 6 per group).

Statistical analysis

Data were analyzed by a two-tailed student's *t*-test or one-way analysis of variance (ANOVA) to initially determine whether an overall statistically significant change existed before using Tukey's *post hoc* test. For all graphs, data are represented as mean ± SEM. A *p*-value less than 0.05 was considered statistically significant.

Results

Generation of osteocytic ERα deletion mice

To investigate the function of ERα in osteocytes, we generated mice lacking ERα in late-osteoblasts/osteocytes by crossing ERα floxed mice with Dmp1-Cre mice, which express Cre recombinase driven by the Dmp1 promoter. The mice harboring the genotypes of *Dmp1*^{Cre}; *ERα*$^{L2/L2}$ and *ERα*$^{L2/L2}$ were analyzed as *ERα*$^{\Delta Ocy/\Delta Ocy}$ and *ERα*$^{flox/flox}$, respectively. First, to assess cell type specificity of the deletion of the ERα gene locus by Dmp1 promoter-driven Cre recombinase, genomic PCR was performed using DNA extracted from *ERα*$^{\Delta Ocy/\Delta Ocy}$. As a result, a relatively specific deletion of ERα in osteocytes, which were isolated by sequential enzymatic digestion, was detected as an L-band, which was seen only in osteocytes and not in primary cultured osteoblasts or osteoclasts (Fig. 1A). In addition, the ERα mRNA level was examined by qPCR using RNA extracted from femoral bones and GFP-mediated FACS sorted osteocytes of *ERα*$^{\Delta Ocy/\Delta Ocy}$ and *ERα*$^{flox/flox}$ mice. As a result, there was an approximately 30% and 90% reduction of ERα expression in whole bone and osteocytes, respectively, in *ERα*$^{\Delta Ocy/\Delta Ocy}$ compared to *ERα*$^{flox/flox}$ mice (Fig. 1B). This significant but low percent deletion in whole bone might reflect ERα expression by other cell types, which are present in the intact femur even though the bone marrow was removed. Also, one group reported that clear deletion of the target gene was detected at the genome level but not the mRNA level when using the Dmp1-Cre mice [42]. Next, body weight was measured

every other week from 3 to 12 weeks old. There was no significant difference in body weight between *ERα*$^{\Delta Ocy/\Delta Ocy}$ and *ERα*$^{flox/flox}$, whereas it was previously reported that ERα total KO mice exhibited a significant increase in body weight [43] (Fig. 1C). Next, we asked if these mice could be a suitable model for analyzing ERα function without the systemic influence of hormones (endocrine disturbances) as described in the conventional ERα null mouse, by examining the concentration of sex steroid hormones. Serum estradiol, testosterone and luteinizing hormone concentrations were measured by ELISA, showing that there were no significant differences between the 12-week-old *ERα*$^{\Delta Ocy/\Delta Ocy}$ and *ERα*$^{flox/flox}$, regardless of gender (Fig. 1D). Since *ERα*$^{\Delta Ocy/\Delta Ocy}$ mice exhibited a relatively specific deletion of ERα in osteocytes and normal serum sex steroid hormone levels, we concluded that *ERα*$^{\Delta Ocy/\Delta Ocy}$ could be used for analysis of ERα function in osteocytes without the complications of endocrine disturbances.

Osteocytic ERα deletion female mice exhibit an osteopenic phenotype

The BMD of 12-week-old *ERα*$^{\Delta Ocy/\Delta Ocy}$ and *ERα*$^{flox/flox}$ were measured by DXA, showing that the BMD of female *ERα*$^{\Delta Ocy/\Delta Ocy}$ was significantly decreased in the proximal, not in middle and distal, tibiae compared to that of female *ERα*$^{flox/flox}$ (Fig. 1E). However, the BMD of tibiae from male *ERα*$^{\Delta Ocy/\Delta Ocy}$ were not significantly different from that of male *ERα*$^{flox/flox}$ (Fig. 1E). Next, to assess changes in bone structure between female *ERα*$^{\Delta Ocy/\Delta Ocy}$ and *ERα*$^{flox/flox}$ mice, μCT analysis was performed. Decreased trabecular bone mass in *ERα*$^{\Delta Ocy/\Delta Ocy}$ mice was observed by μCT analysis (Fig. 2A). Trabecular bone of female *ERα*$^{\Delta Ocy/\Delta Ocy}$ exhibited a significant decrease in BV/TV, vBMD, Tb.N and Conn-D, and an increase in Tb.Sp and SMI compared to those of female *ERα*$^{flox/flox}$ (Fig. 2B). The parameters in metaphyseal cortical bone of female *ERα*$^{\Delta Ocy/\Delta Ocy}$ were not significantly different from that of female *ERα*$^{flox/flox}$ (Fig. 2C).

Osteocytic ERα regulates bone formation through control of osteoblasts

To examine whether the reduced bone phenotype of *ERα*$^{\Delta Ocy/\Delta Ocy}$ could be caused by alterations in the potential interaction between osteocytes and either osteoblasts or osteoclasts, bone histomorphometry was performed. The number and/or activity of osteoblasts/osteoclasts were examined in *ERα*$^{\Delta Ocy/\Delta Ocy}$ and *ERα*$^{flox/flox}$, using lumbar vertebrae of 12-week-old female *ERα*$^{\Delta Ocy/\Delta Ocy}$ and *ERα*$^{flox/flox}$. Parameters related to osteoblastic bone formation, such as N.Ob/B.Pm and Ob.S/BS, were significantly decreased in *ERα*$^{\Delta Ocy/\Delta Ocy}$ compared to *ERα*$^{flox/flox}$ (Fig. 3). In addition, N.Ocy/B.Ar was also decreased in *ERα*$^{\Delta Ocy/\Delta Ocy}$, which might be due to a decreased number of osteoblasts, which are precursors of osteocytes. Also, the reduction of BFR/BS and MAR in *ERα*$^{\Delta Ocy/\Delta Ocy}$ tended to be significant ($p = 0.07$), due to the reduction of osteoblastic parameters. On the other hand, parameters related to osteoclastic bone resorption, such as N.Oc/B.Pm and Oc.S/BS, were not altered in *ERα*$^{\Delta Ocy/\Delta Ocy}$ when compared to *ERα*$^{flox/flox}$ (Fig. 3). These results suggested that deficiency of ERα in osteocytes could decrease the number of osteoblasts and consequently their bone forming activity, indicating that bone mass reduction in *ERα*$^{\Delta Ocy/\Delta Ocy}$ could be caused by a reduction of osteoblastic bone formation, not a promotion of osteoclastic bone resorption. In addition, this result implies that osteocytic ERα might positively regulate osteoblastic bone formation by signaling from osteocytes, such as in a paracrine manner or by cell–cell contact.

Gene expression profiles of osteocytes lacking ERα

To determine what secretory proteins or signaling pathways ERα may utilize in osteocytes, a gene array analysis of Dmp1-GFP-positive cells from controls and mice with a targeted deletion of ERα in osteocytes was performed. Dmp1-GFP mice were crossed with *Dmp1*$^{Tg/0}$; *ERα*$^{L2/L2}$ mice to generate *Dmp1-GFP+*; *Dmp1*$^{Tg/0}$; *ERα*$^{L2/+}$ mice, and then *Dmp1-GFP+*; *Dmp1*$^{Tg/0}$; *ERα*$^{L2/L2}$ (*Dmp1-GFP+*; *ERα*$^{\Delta Ocy/\Delta Ocy}$) and
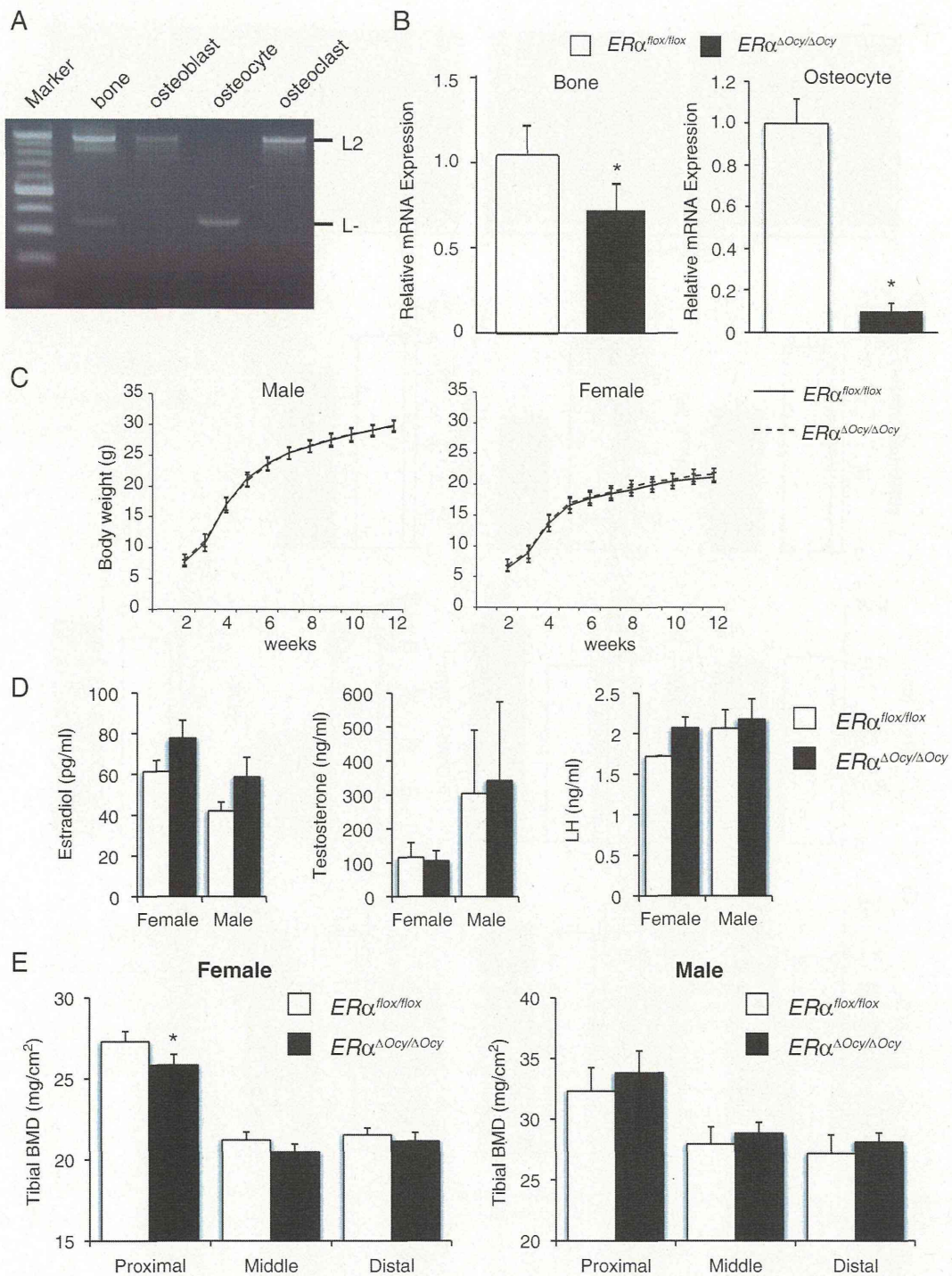
Fig. 1. Generation of mice with targeted deletion of ERα in osteocytes. (A) Deletion of ERα gene locus in osteocyte was detected by genome PCR in $ERα^{\Delta Ocy/\Delta Ocy}$. (B) mRNA levels of ERα from whole femurs (left panel) and isolated osteocytes (right panel) of $ERα^{flox/flox}$ and $ERα^{\Delta Ocy/\Delta Ocy}$ mice was evaluated by RT-qPCR. Data are represented as mean ± SEM (n = 3). (C) The growth curves of $ERα^{flox/flox}$ and $ERα^{\Delta Ocy/\Delta Ocy}$ mice. Data are represented as mean ± SEM (n = 7–10). (D) Serum hormone levels of 12-week-old $ERα^{flox/flox}$ and $ERα^{\Delta Ocy/\Delta Ocy}$ mice. Data are represented as mean ± SEM (n = 4–7). (E) BMD of 1/3 portion of longitudinal divisions of tibiae from 12-week-old $ERα^{flox/flox}$ and $ERα^{\Delta Ocy/\Delta Ocy}$ mice. Data are represented as mean ± SEM (Female n = 8, Male n = 7). * indicates $p < 0.05$.

$Dmp1$-$GFP+$; $ERα^{L2/L2}$ ($Dmp1$-$GFP+$; $ERα^{flox/flox}$) were generated by crossing $Dmp1$-$GFP+$; $Dmp1^{Tg/0}$; $ERα^{L2/+}$ and $ERα^{L2/L2}$. Calvariae obtained from approximately 10-day-old female $Dmp1$-$GFP+$; $ERα^{\Delta Ocy/\Delta Ocy}$ and $Dmp1$-$GFP+$; $ERα^{flox/flox}$ were treated with sequential enzymatic digestion and subjected to FACS. The percentage of GFP+ cells in fractions

4 to 6 was increased compared to that in fractions 2 to 4 (23.3% and 8.2%, respectively) (Fig. 4A). To determine if osteocytes were highly purified in this system, gene expression of cell-type specific marker genes in GFP+ cells (osteocytes) and GFP− cells (osteoblasts) was confirmed by RT-qPCR. As a result, the expression of Dmp1 (osteocyte marker
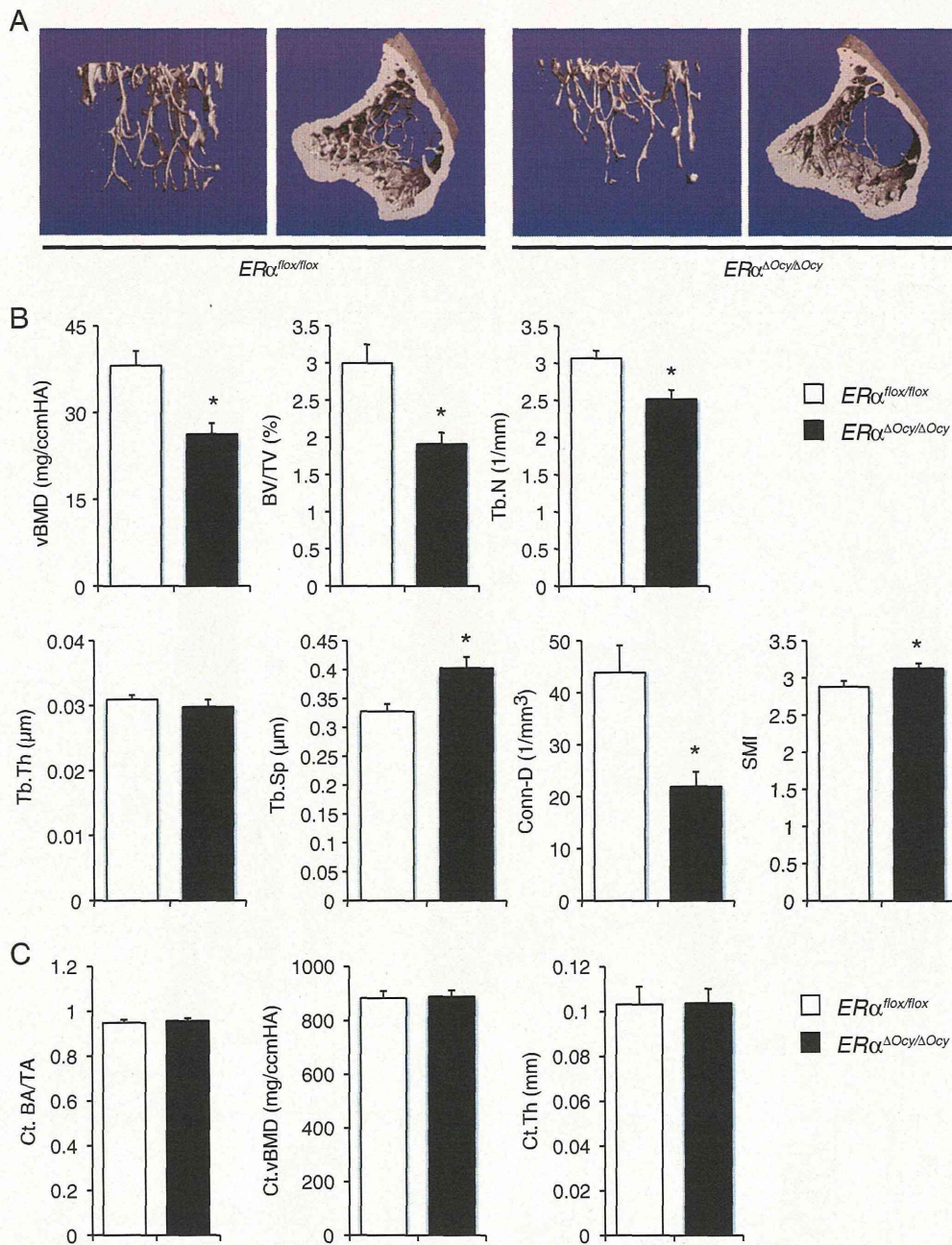
Fig. 2. μCT analyses of the mice lacking ERα in osteocytes. (A) Representative μCT views. (B) 3D measurements of proximal tibiae from $ER\alpha^{flox/flox}$ and $ER\alpha^{\Delta Ocy/\Delta Ocy}$ mice. Data are represented as mean ± SEM (n = 10). * indicates $p < 0.05$.

gene) in GFP+ cells was about 25 times higher than in GFP− cells, while the expression of keratocan, Kera, (osteoblast marker gene) in GFP− cells was about 25 times higher than in GFP+ cells (Fig. 4B). Extracted total RNA from $Dmp1$-GFP+; $ER\alpha^{\Delta Ocy/\Delta Ocy}$ (n = 3) and $Dmp1$-GFP+; $ER\alpha^{flox/flox}$ (n = 3) was subjected to a gene expression microarray analysis with GeneChip Mouse Genome 430 2.0 (Affymetrix). There were 276 genes found to be significantly differentially expressed between $ER\alpha^{\Delta Ocy/\Delta Ocy}$ and $ER\alpha^{flox/flox}$ ($p < 0.01$). Among them, 76 genes were significantly down-regulated and 200 genes were up-regulated (Fig. 4C). Gene ontology analyses revealed that 'secreted' was listed top in the Keyword analysis when sorted by p-value (Fig. 4D). Among

these genes, Mdk (Midkine) and $Sostdc1$ (Sclerostin domain containing 1) were significantly up-regulated in $ER\alpha^{\Delta Ocy/\Delta Ocy}$ although there were no significant differences in $Sost$ or β-catenin ($Ctnnb1$) gene expression (Fig. 4E). Up-regulation of mRNA of Mdk and $Sostdc1$ in $ER\alpha^{\Delta Ocy/\Delta Ocy}$ was also validated when determined by RT-qPCR (Fig. 4F). From the results of functional annotation in differentially expressed genes between $ER\alpha^{\Delta Ocy/\Delta Ocy}$ and $ER\alpha^{flox/flox}$, osteocytic ERα could regulate the expression of secretory protein genes such as Mdk and $Sostdc1$, which have been shown to be inhibitors of Wnt signaling-related bone formation [44–46]. However, the expression levels of Mdk and $Sostdc1$ were not significantly altered when late-stage primary cultured osteoblasts
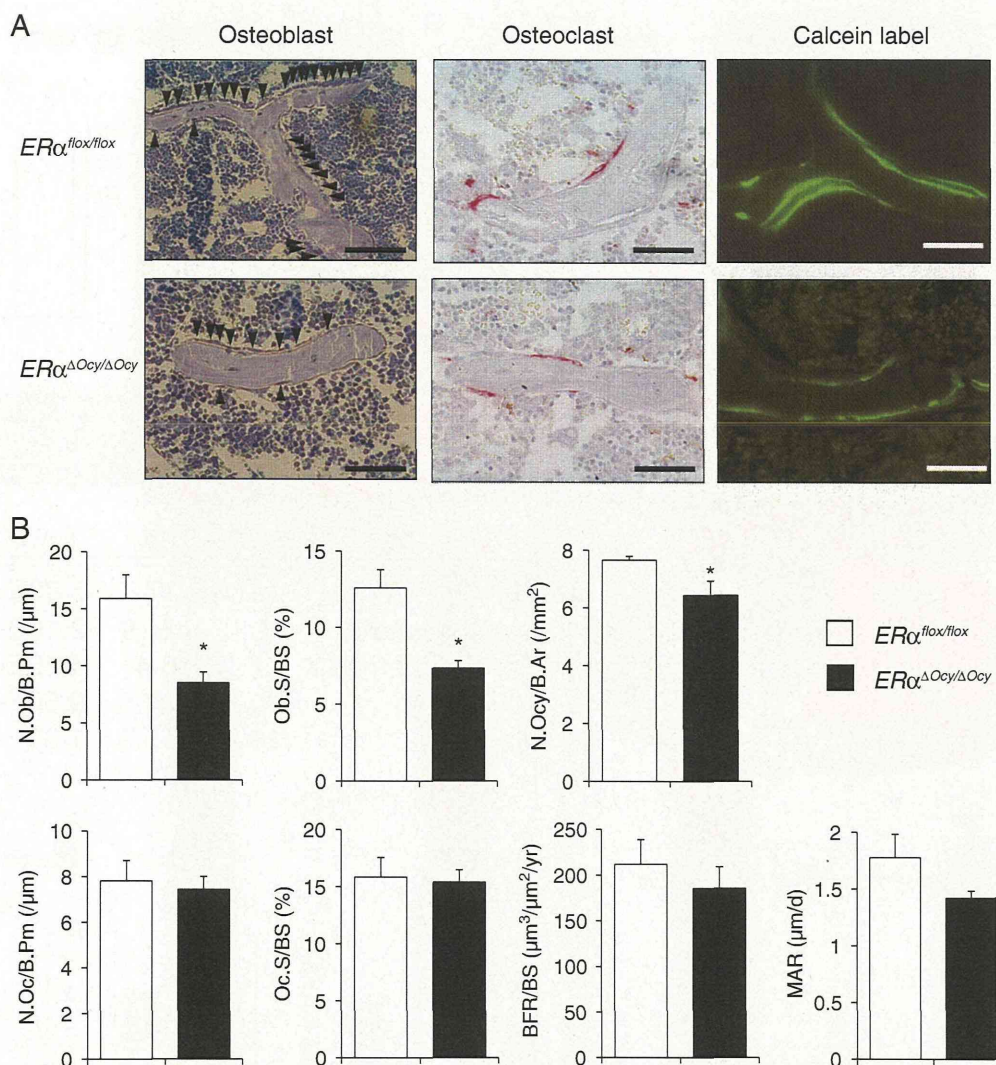
Fig. 3. ERα$^{\Delta Ocy/\Delta Ocy}$ mice exhibit decreased bone formation. (A) Representative views of Toluidine blue staining for mononuclear cuboidal osteoblasts (arrowhead), TRAP staining for multinuclear TRAP-positive osteoclasts and calcein labeling for dynamic parameters are shown. Bars indicate 50 μm. (B) Data are represented as mean ± SEM (n = 6). * indicates p < 0.05.

were treated with 17β-estradiol for 2 or 6 h (Supplemental Fig. S1), indicating that *Mdk* and *Sostdc1* might not be early responsive genes, but be indirect target genes.

Trabecular bone loss is exacerbated in ERα$^{\Delta Ocy/\Delta Ocy}$ in response to unloading while cortical bone is resistant to unloading-induced bone loss

ERα has been reported to be involved in mechanosensing and increasing cortical bone formation under overloading conditions [11]. The hindlimb tail suspension model is a well-known model for unloading (or immobilization) and it is also reported that tail suspension-induced bone loss is significantly enhanced by ovariectomy [47]. To determine whether osteocytic ERα plays any roles in unloading-induced bone loss, a hindlimb suspension experiment was performed for female ERα$^{\Delta Ocy/\Delta Ocy}$ and ERα$^{flox/flox}$ for 4 weeks starting at 8 weeks of age. Control mice were chained to the cage top during the same period but allowed to load their hindlimbs to control for stress related effects.

During the 4-week experimental period, the average body weight of the experimental group increased 1 g, whereas the control group increased 2 g (Supplemental Fig. S2). Although there was a significant difference in body weight increase over the four weeks between the experimental and control groups, there was no significant difference

in body weight between ERα$^{\Delta Ocy/\Delta Ocy}$ and ERα$^{flox/flox}$ within each group at the end of the experiment (Supplemental Fig. S2). Femoral diaphysis and distal metaphysis of the unloaded and loaded groups of both genotypes (ERα$^{\Delta Ocy/\Delta Ocy}$ and ERα$^{flox/flox}$) were measured using μCT. vBMD in the femoral diaphysis of tail suspended female ERα$^{\Delta Ocy/\Delta Ocy}$ was significantly higher than that of ERα$^{flox/flox}$ (Figs. 5A and B), although there were no significant differences in bone area or cortical thickness between genotypes. Upon further analysis, it was found that the trabecular bone mass was decreased in unloaded mice regardless of genotypes, and tail suspension induced trabecular bone loss in ERα$^{\Delta Ocy/\Delta Ocy}$ was greater than that in ERα$^{flox/flox}$ (Figs. 5C and D). These data indicate that osteocytic ERα is protective against trabecular bone loss due to unloading.

Discussion

Based on reports on the functions of ERα in bone, estrogens are osteoprotective by regulating the life span of osteoclasts through osteoclastic and osteoblastic ERα and also by inhibiting apoptosis of osteoblasts and osteocytes [8,9,48–50]. Recently, it was reported that osteoblastic ERα has an osteoprotective function [12,14,15], however, little is known about the role of osteocytes in the osteoprotective actions
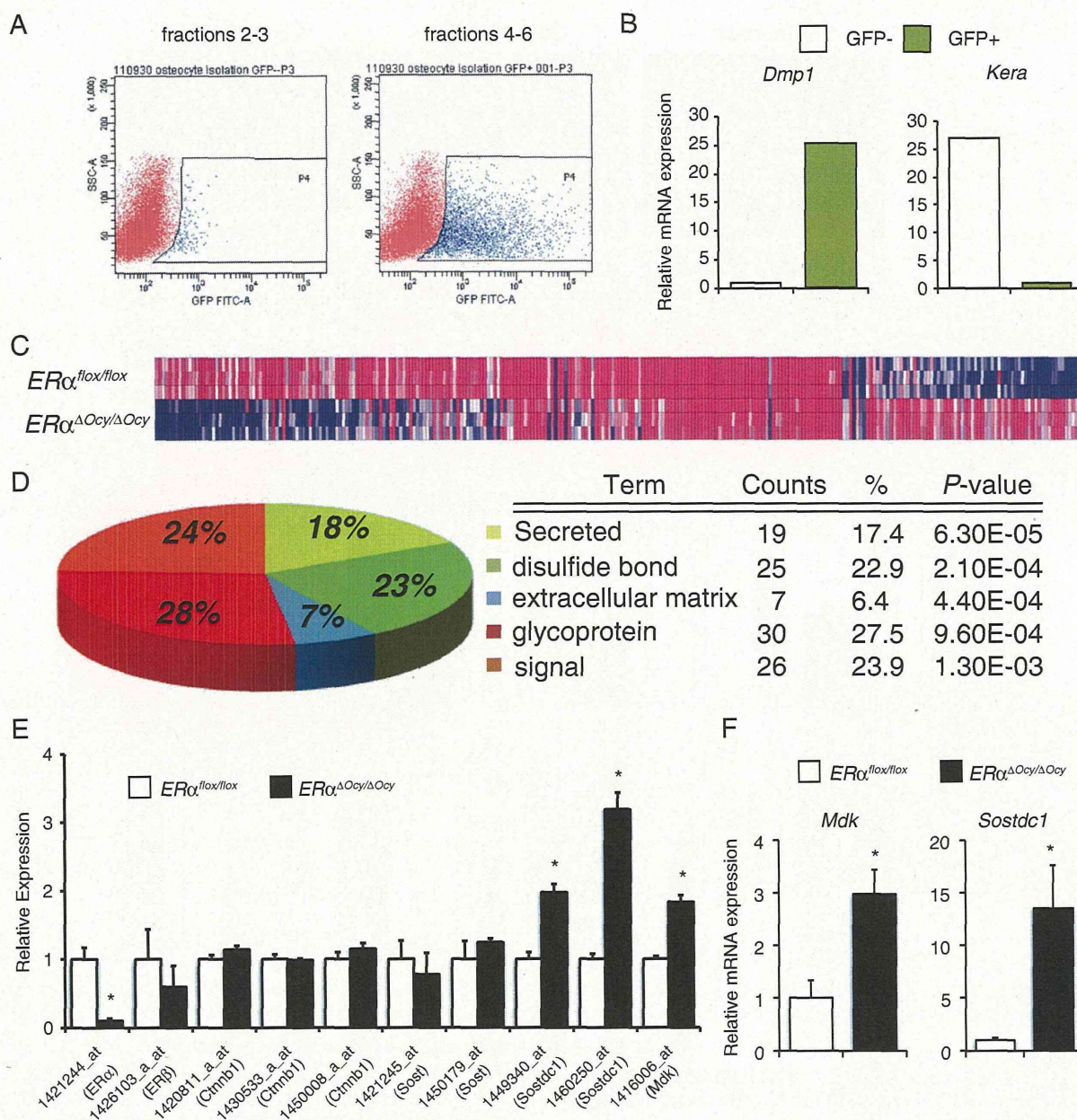
Fig. 4. Osteocytes lacking ERα show increased Mdk and Sostdc1 expression. (A) Two-dimensional dot plot of cells obtained from sequential enzymatic digestion of calvariae of mice expressing Dmp1-GFP. Left: fractions 2–3, right: fractions 4–6. (B) Expression of osteocyte (Dmp1) and osteoblast (Kera) marker genes in the GFP− and GFP+ population of isolated cells. (C) Heat map of significantly regulated genes in the gene expression microarray using total RNA from isolated GFP+ cells of ERα$^{flox/flox}$ and ERα$^{\Delta Ocy/\Delta Ocy}$ mice harboring Dmp1-GFP (n = 3). Red: high expression. Blue: low expression. (D) Functional annotation clustering of Keywords by DAVID Bioinformatic Resources. (E) Relative microarray intensity of each probe for ERα, ERβ, Ctnnb1 (β-catenin), Sost, Sostdc1 and Mdk. Data are represented as mean ± SEM (n = 3). (F) RT-qPCR for Mdk and Sostdc1 as same as panel E. * indicates p < 0.05.

of estrogens in skeletal homeostasis. To decipher the direct functions of ERα in osteocytes, the most abundant bone cell type in the adult skeleton, mice lacking ERα in osteocytes were genetically generated and their bone phenotype were analyzed in this study. ERα in osteocytes was found to play a significant role in maintaining bone mass by regulating osteoblastic bone formation only in females. It was further revealed that ERα in osteocytes is supportive for maintaining trabecular bone mass not only under normal loading conditions but also under tail suspension-induced unloading, which can be considered as experimental recapitulation of immobilization or space flight. However, the absence of this receptor protected against cortical bone loss. These results are consistent with a previous report in which bone mass adaptation induced by

mechanical loading was impaired in ERα null mice [11]. Together, these results indicate that osteocyte mechanosensations at least in part via osteocytic ERα.

Maatta et al. and Melville et al. suggested that ERα in mature osteoblasts plays a role in maintaining trabecular bone mass in females based on analyses of mice lacking ERα in mature osteoblasts using Osteocalcin-Cre mice [12,15]. Almeida et al. suggested that ERα in osteoblast progenitors, but not in mature osteoblasts or osteocytes, is essential for regulation of female cortical bone [14]. As mentioned above, the functions of ERα in osteoblast lineage cells in vivo are still controversial and it is important to combine knowledge from various studies. All female mice exhibited an osteopenic phenotype in both the osteoblast-specific ERα
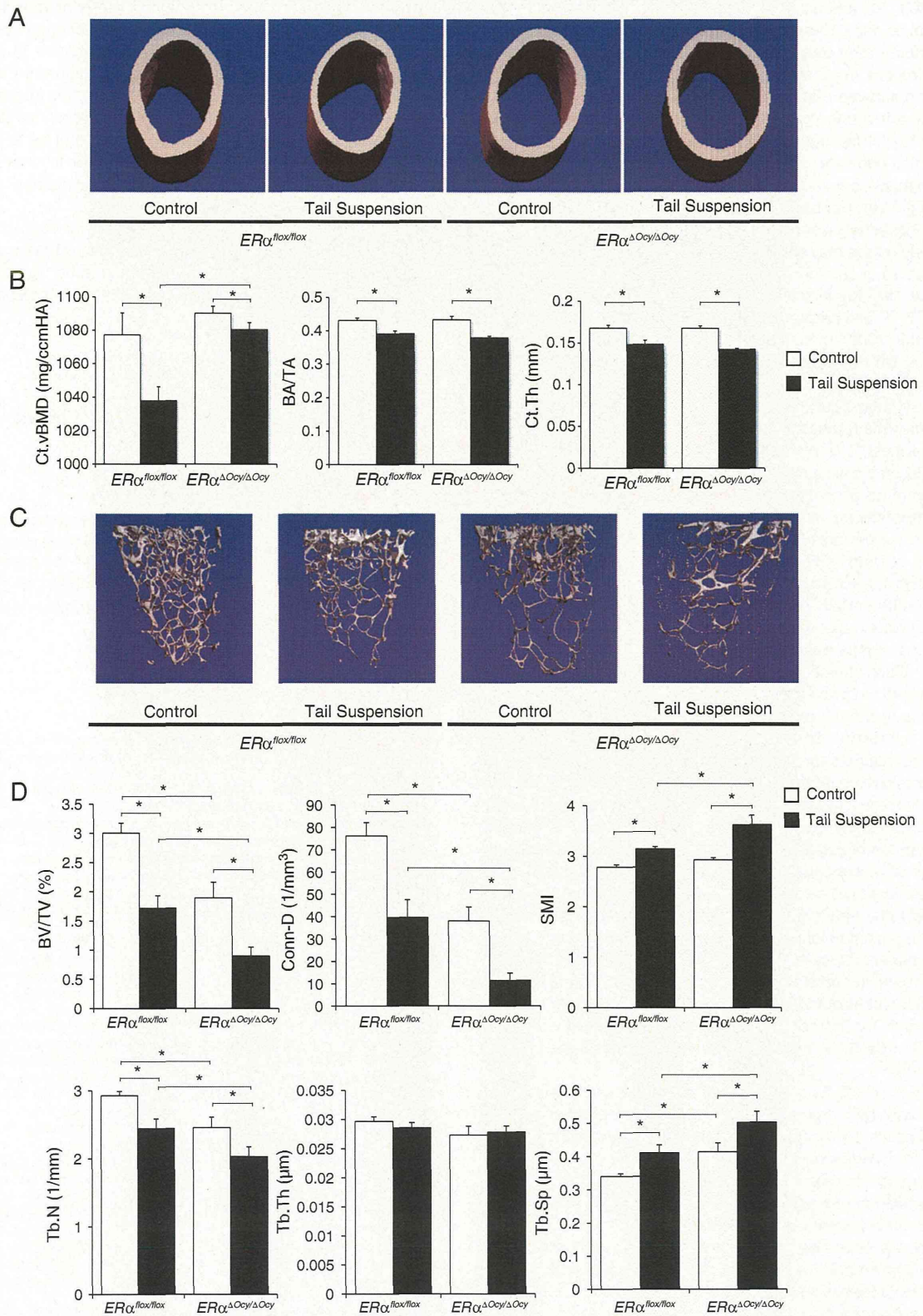
Fig. 5. Effects of unloading on trabecular and cortical bone in mice with targeted deletion of ERα in osteocytes. (A and C) Representative μCT views. (B) 3D measurements of femoral distal trabecular area and (D) 3D measurements of femoral diaphyses from $ER\alpha^{flox/flox}$ and $ER\alpha^{\Delta Ocy/\Delta Ocy}$ mice subjected or not subjected to tail suspension. Data are represented as mean $\pm$ SEM (n = 6). * indicates $p < 0.05$.

knockout mice by Maatta et al. and Almeida et al., and in previous reports regarding osteoclast-specific ERα knockout mice [8,9]. As would be predicted, androgen receptor knockout mice (ARKO), including both systemic ARKO [51] and osteocyte conditional ARKO [52], exhibited bone loss in male mice. These gender-specific phenotypes are probably caused by differences in concentration of circulating sex steroids, estrogens and androgens. In contrast to these studies and our present study, a recent report showed that mice lacking ERα using the same Dmp1-Cre mouse exhibited trabecular bone loss only in male mice, but not in female mice [13]. In this report, Windahl et al. proposed that the physiological trabecular bone-sparing effect of estrogen is mediated via ERα in osteocytes in males, but also via ERα in osteoclasts in females [13]. At present, it is difficult to provide a convincing explanation to describe the discrepancies between our current study and this report [13]. However, one possible reason may be differences in the genetic background of the mouse strain of the ERα-floxed mice since the Dmp1-Cre mice were identical. The ERα-floxed mice used in our study have been registered as $Esr1^{tm1Mma}$ and originated from 129S2/SvPas mixed background, and published in 2000 [5], then backcrossed with C57BL6 line for more than 10 times. On the other hand, the ERα-floxed mice used in the study by Windahl et al. have been registered as $Esr1^{tm1Gust}$ and originated from 129X1/SvJ mixed background, and published in 2012 [53]. These differences might be responsible for the discrepancies between the two studies. Regardless, the results of these two studies suggest that osteocytic ERα may have a role in maintenance of trabecular bone homeostasis regardless of gender.

To investigate the possible molecular basis underlying ERα function in osteocytes, we performed an osteocyte isolation technique using FACS analysis of Dmp1-GFP positive cells from conditional null mice and their controls. The results obtained from the Functional Annotation Clustering of differentially expressed genes suggested that osteocytic ERα might regulate transcription of the genes related to secretory proteins, which may regulate osteoblastic bone formation and contribute to maintenance of bone homeostasis. In fact, Sostdc1, an antagonist of the Wnt signaling [45,54], was elevated as a downstream gene of osteocytic ERα. Sostdc1 is a gene also called Wise or Ectodin whose domain is similar to Sost (Sclerostin). Sost and Sostdc1 bind to Wnt co-receptors called Lrps and regulate the Wnt/β-catenin pathway negatively [55]. Wnt signal proteins are reported to modulate bone mass in vivo by acting directly on mesenchymal stem cells [56–59]. Genes involved in the Wnt signaling are known to regulate the cell proliferation, differentiation, and apoptosis of osteoblasts [60]. Interaction between β-catenin and ERα has been previously reported [61] and the expressions of some Wnt family genes are important for responding to mechanical stress and are reportedly regulated by ERα [32]. Conventional Sostdc1 KO mice are reported to exhibit abnormal tooth development, which has similar characteristics as bone [45,54]. Also, it has been reported that estradiol regulates mRNA levels of Sostdc1 in U2OS cells [62]. In addition, a meta-analysis of BMD in a female Chinese population revealed that a mutation in the Sostdc1 cording region was correlated with BMD, suggesting that Sostdc1 might play a role in homeostasis of bone metabolism [46].

Also, Midkine, Mdk, was elevated as a downstream molecule of ERα in mice with this targeted deletion. Mdk is a member of a family of heparin-binding growth factors known primarily for their effects on neural cells [63]. Mdk expression is reported to increase during the course of primary osteoblast differentiation. Mdk has been shown to bind to a complex of protein tyrosine phosphatase zeta (Ptprx), low-density lipoprotein receptor-related protein-6 (Lrp6), and exert negative effects on Wnt signaling [64]. Conventional Mdk null mice exhibit increased bone formation, suggesting Mdk is a negative regulator of osteoblastic bone formation. Furthermore, Mdk KO mice are resistant to OVX-induced bone loss and sensitive to mechanical loading induced cortical bone increase [44]. In addition, the expression of ALP and the induction of canonical Wnt signaling in MC3T3E1, an osteoblastic cell line, were inhibited by Mdk treatments [64]. These reports and the results

from our current study suggest that Sostdc1 and Mdk might be responsible for a component of estrogen's osteoprotective actions.

However, questions remain regarding how ERα negatively regulates the transcription of these genes because there are no reports of a negative transcriptional regulation of the estrogen receptor response element (negative ERE), although details of a negative glucocorticoid receptor response element (nGRE) have been reported [65]. Alternatively, it is possible that the expression of these factors might be regulated by an ERα-dependent miRNA. The precise molecular basis of transcriptional regulation or mRNA stabilization of these genes must be clarified in future studies. Neutralizing or deletion studies of these two proteins in this mouse model could provide possible answers for these questions.

In conclusion, osteocytic ERα might play a role in estrogen's osteoprotective action by controlling the expression of Wnt antagonists, which regulate osteoblastic bone formation in trabecular bone.

Supplementary data to this article can be found online at http://dx.doi.org/10.1016/j.bone.2013.12.005.

Conflict of interest

All authors state that they have no conflicts of interest.

Acknowledgments

References

[1] Nelson HD. Menopause. Lancet 2008;371:760–70.
[2] Imai Y, Kondoh S, Kouzmenko A, Kato S. Minireview: osteoprotective action of estrogens is mediated by osteoclastic estrogen receptor-alpha. Mol Endocrinol 2010;24:877–85.
[3] Sun L, Peng Y, Sharrow AC, Iqbal J, Zhang Z, Papachristou DJ, et al. FSH directly regulates bone mass. Cell 2006;125:247–60.
[4] Pacifici R. Estrogen deficiency, T cells and bone loss. Cell Immunol 2008;252:68–80.
[5] Dupont S, Krust A, Gansmuller A, Dierich A, Chambon P, Mark M. Effect of single and compound knockouts of estrogen receptors alpha (ERalpha) and beta (ERbeta) on mouse reproductive phenotypes. Development 2000;127:4277–91.
[6] Windahl SH, Andersson G, Gustafsson JA. Elucidation of estrogen receptor function in bone with the use of mouse models. Trends Endocrinol Metab 2002;13:195–200.
[7] Sims NA, Dupont S, Krust A, Clement-Lacroix P, Minet D, Resche-Rigon M, et al. Deletion of estrogen receptors reveals a regulatory role for estrogen receptors-beta in bone remodeling in females but not in males. Bone 2002;30:18–25.
[8] Nakamura T, Imai Y, Matsumoto T, Sato S, Takeuchi K, Igarashi K, et al. Estrogen prevents bone loss via estrogen receptor alpha and induction of Fas ligand in osteoclasts. Cell 2007;130:811–23.
[9] Martin-Millan M, Almeida M, Ambrogini E, Han L, Zhao H, Weinstein RS, et al. The estrogen receptor-alpha in osteoclasts mediates the protective effects of estrogens on cancellous but not cortical bone. Mol Endocrinol 2010;24:323–34.
[10] Tomkinson A, Reeve J, Shaw RW, Noble BS. The death of osteocytes via apoptosis accompanies estrogen withdrawal in human bone. J Clin Endocrinol Metab 1997;82:3128–35.
[11] Lee K, Jessop H, Suswillo R, Zaman G, Lanyon L. Endocrinology: bone adaptation requires oestrogen receptor-alpha. Nature 2003;424:389.
[12] Maatta JA, Buki KG, Gu G, Alanne MH, Vaaraniemi J, Liljenback H, et al. Inactivation of estrogen receptor alpha in bone-forming cells induces bone loss in female mice. FASEB J 2012;27:478–88.
[13] Windahl SH, Borjesson AE, Farman HH, Engdahl C, Moverare-Skrtic S, Sjogren K, et al. Estrogen receptor-alpha in osteocytes is important for trabecular bone formation in male mice. Proc Natl Acad Sci U S A 2013;110:2294–9.
[14] Almeida M, Iyer S, Martin-Millan M, Bartell SM, Han L, Ambrogini E, et al. Estrogen receptor-alpha signaling in osteoblast progenitors stimulates cortical bone accrual. J Clin Invest 2013;123:394–404.
[15] Melville KM, Kelly NH, Khan SA, Schimenti JC, Ross FP, Main RP, et al. Female mice lacking estrogen receptor-alpha in osteoblasts have compromised bone mass and strength. J Bone Miner Res 2013 (in press) (Epub ahead of print).
[16] Burger EH, Klein-Nulend J. Mechanotransduction in bone—role of the lacuno-canalicular network. FASEB J 1999(13 Suppl.):S101–12.

[17] Robling AG, Niziolek PJ, Baldridge LA, Condon KW, Allen MR, Alam I, et al. Mechanical stimulation of bone in vivo reduces osteocyte expression of Sost/sclerostin. J Biol Chem 2008;283:5866–75.

[18] Skerry TM, Bitensky L, Chayen J, Lanyon LE. Early strain-related changes in enzyme activity in osteocytes following bone loading in vivo. J Bone Miner Res 1989;4:783–8.

[19] Gluhak-Heinrich J, Ye L, Bonewald LF, Feng JQ, MacDougall M, Harris SE, et al. Mechanical loading stimulates dentin matrix protein 1 (DMP1) expression in osteocytes in vivo. J Bone Miner Res 2003;18:807–17.

[20] Gluhak-Heinrich J, Pavlin D, Yang W, MacDougall M, Harris SE. MEPE expression in osteocytes during orthodontic tooth movement. Arch Oral Biol 2007;52:684–90.

[21] Thompson DL, Sabbagh Y, Tenenhouse HS, Roche PC, Drezner MK, Salisbury JL, et al. Ontogeny of Phex/PHEX protein expression in mouse embryo and subcellular localization in osteoblasts. J Bone Miner Res 2002;17:311–20.

[22] Nampei A, Hashimoto J, Hayashida K, Tsuboi H, Shi K, Tsuji I, et al. Matrix extracellular phosphoglycoprotein (MEPE) is highly expressed in osteocytes in human bone. J Bone Miner Metab 2004;22:176–84.

[23] Liu S, Zhou J, Tang W, Jiang X, Rowe DW, Quarles LD. Pathogenic role of Fgf23 in Hyp mice. Am J Physiol Endocrinol Metab 2006;291:E38–49.

[24] Feng JQ, Ward LM, Liu S, Lu Y, Xie Y, Yuan B, et al. Loss of DMP1 causes rickets and osteomalacia and identifies a role for osteocytes in mineral metabolism. Nat Genet 2006;38:1310–5.

[25] Bonewald LF. Osteocytes as dynamic multifunctional cells. Ann N Y Acad Sci 2007;1116:281–90.

[26] Bergmann P, Body JJ, Boonen S, Boutsen Y, Devogelaer JP, Goemaere S, et al. Loading and skeletal development and maintenance. J Osteoporos 2010;2011:786752.

[27] Lloyd SA, Bandstra ER, Willey JS, Riffle SE, Tirado-Lee L, Nelson GA, et al. Effect of proton irradiation followed by hindlimb unloading on bone in mature mice: a model of long-duration spaceflight. Bone 2012;51:756–64.

[28] Lee KC, Maxwell A, Lanyon LE. Validation of a technique for studying functional adaptation of the mouse ulna in response to mechanical loading. Bone 2002;31:407–12.

[29] Bonewald LF, Johnson ML. Osteocytes, mechanosensing and Wnt signaling. Bone 2008;42:606–15.

[30] Robinson JA, Chatterjee-Kishore M, Yaworsky PJ, Cullen DM, Zhao W, Li C, et al. Wnt/beta-catenin signaling is a normal physiological response to mechanical loading in bone. J Biol Chem 2006;281:31720–8.

[31] Javaheri B, Stern A, Lara N, Dallas M, Zhao H, Liu Y, et al. Deletion of a single beta-catenin allele in osteocytes abolishes the bone anabolic response to loading. J Bone Miner Res 2013 (in press) (Epub ahead of print).

[32] Armstrong VJ, Muzylak M, Sunters A, Zaman G, Saxon LK, Price JS, et al. Wnt/beta-catenin signaling is a component of osteoblastic bone cell early responses to load-bearing and requires estrogen receptor alpha. J Biol Chem 2007;282:20715–27.

[33] Lu Y, Xie Y, Zhang S, Dusevich V, Bonewald LF, Feng JQ. DMP1-targeted Cre expression in odontoblasts and osteocytes. J Dent Res 2007;86:320–5.

[34] Kalajzic I, Braut A, Guo D, Jiang X, Kronenberg MS, Mina M, et al. Dentin matrix protein 1 expression during osteoblastic differentiation, generation of an osteocyte GFP-transgene. Bone 2004;35:74–82.

[35] Bouxsein ML, Boyd SK, Christiansen BA, Guldberg RE, Jepsen KJ, Muller R. Guidelines for assessment of bone microstructure in rodents using micro-computed tomography. J Bone Miner Res 2010;25:1468–86.

[36] Sato S, Hanada R, Kimura A, Abe T, Matsumoto T, Iwasaki M, et al. Central control of bone remodeling by neuromedin U. Nat Med 2007;13:1234–40.

[37] Parfitt AM, Drezner MK, Glorieux FH, Kanis JA, Malluche H, Meunier PJ, et al. Bone histomorphometry: standardization of nomenclature, symbols, and units. Report of the ASBMR Histomorphometry Nomenclature Committee. J Bone Miner Res 1987;2:595–610.

[38] Paic F, Igwe JC, Nori R, Kronenberg MS, Franceschetti T, Harrington P, et al. Identification of differentially expressed genes between osteoblasts and osteocytes. Bone 2009;45:682–92.

[39] Huang da W, Sherman BT, Lempicki RA. Systematic and integrative analysis of large gene lists using DAVID bioinformatics resources. Nat Protoc 2009;4:44–57.

[40] McCarthy JJ, Fox AM, Tsika GL, Gao L, Tsika RW. Beta-MHC transgene expression in suspended and mechanically overloaded/suspended soleus muscle of transgenic mice. Am J Physiol 1997;272:R1552–61.

[41] Tsika G, Ji J, Tsika R. Sp3 proteins negatively regulate beta myosin heavy chain gene expression during skeletal muscle inactivity. Mol Cell Biol 2004;24:10777–91.

[42] Xiong J, Onal M, Jilka RL, Weinstein RS, Manolagas SC, O'Brien CA. Matrix-embedded cells control osteoclast formation. Nat Med 2011;17:1235–41.

[43] Heine PA, Taylor JA, Iwamoto GA, Lubahn DB, Cooke PS. Increased adipose tissue in male and female estrogen receptor-alpha knockout mice. Proc Natl Acad Sci U S A 2000;97:12729–34.

[44] Neunaber C, Catala-Lehnen P, Beil FT, Marshall RP, Kanbach V, Baranowsky A, et al. Increased trabecular bone formation in mice lacking the growth factor midkine. J Bone Miner Res 2010;25:1724–35.

[45] Ahn Y, Sanderson BW, Klein OD, Krumlauf R. Inhibition of Wnt signaling by Wise (Sostdc1) and negative feedback from Shh controls tooth number and patterning. Development 2010;137:3221–31.

[46] He JW, Yue H, Hu WW, Hu YQ, Zhang ZL. Contribution of the sclerostin domain-containing protein 1 (SOSTDC1) gene to normal variation of peak bone mineral density in Chinese women and men. J Bone Miner Metab 2011;29:571–81.

[47] Tou JC, Foley A, Yuan YV, Arnaud S, Wade CE, Brown M. The effect of ovariectomy combined with hindlimb unloading and reloading on the long bones of mature Sprague–Dawley rats. Menopause 2008;15:494–502.

[48] Almeida M, Martin-Millan M, Ambrogini E, Bradsher 3rd R, Han L, Chen XD, et al. Estrogens attenuate oxidative stress and the differentiation and apoptosis of osteoblasts by DNA-binding-independent actions of the ERalpha. J Bone Miner Res 2010;25:769–81.

[49] Tomkinson A, Gevers EF, Wit JM, Reeve J, Noble BS. The role of estrogen in the control of rat osteocyte apoptosis. J Bone Miner Res 1998;13:1243–50.

[50] Krum SA, Miranda-Carboni GA, Hauschka PV, Carroll JS, Lane TF, Freedman LP, et al. Estrogen protects bone by inducing Fas ligand in osteoblasts to regulate osteoclast survival. EMBO J 2008;27:535–45.

[51] Kawano H, Sato T, Yamada T, Matsumoto T, Sekine K, Watanabe T, et al. Suppressive function of androgen receptor in bone resorption. Proc Natl Acad Sci U S A 2003;100:9416–21.

[52] Sinnesael M, Claessens F, Laurent M, Dubois V, Boonen S, Deboel L, et al. Androgen receptor (AR) in osteocytes is important for the maintenance of male skeletal integrity: evidence from targeted AR disruption in mouse osteocytes. J Bone Miner Res 2012;27:2535–43.

[53] Antonson P, Omoto Y, Humire P, Gustafsson JA. Generation of ERalpha-floxed and knockout mice using the Cre/LoxP system. Biochem Biophys Res Commun 2012;424:710–6.

[54] Cho SW, Kwak S, Woolley TE, Lee MJ, Kim EJ, Baker RE, et al. Interactions between Shh, Sostdc1 and Wnt signaling and a new feedback loop for spatial patterning of the teeth. Development 2011;138:1807–16.

[55] Itasaki N, Jones CM, Mercurio S, Rowe A, Domingos PM, Smith JC, et al. Wise, a context-dependent activator and inhibitor of Wnt signalling. Development 2003;130:4295–305.

[56] Liu G, Vijayakumar S, Grumolato L, Arroyave R, Qiao H, Akiri G, et al. Canonical Wnts function as potent regulators of osteogenesis by human mesenchymal stem cells. J Cell Biol 2009;185:67–75.

[57] Takada I, Kouzmenko AP, Kato S. Wnt and PPARgamma signaling in osteoblastogenesis and adipogenesis. Nat Rev Rheumatol 2009;5:442–7.

[58] Augello A, De Bari C. The regulation of differentiation in mesenchymal stem cells. Hum Gene Ther 2010;21:1226–38.

[59] Baron R, Kneissel M. WNT signaling in bone homeostasis and disease: from human mutations to treatments. Nat Med 2013;19:179–92.

[60] Westendorf JJ, Kahler RA, Schroeder TM. Wnt signaling in osteoblasts and bone diseases. Gene 2004;341:19–39.

[61] Kouzmenko AP, Takeyama K, Ito S, Furutani T, Sawatsubashi S, Maki A, et al. Wnt/beta-catenin and estrogen signaling converge in vivo. J Biol Chem 2004;279:40255–8.

[62] Tee MK, Rogatsky I, Tzagarakis-Foster C, Cvoro A, An J, Christy RJ, et al. Estradiol and selective estrogen receptor modulators differentially regulate target genes with estrogen receptors alpha and beta. Mol Biol Cell 2004;15:1262–72.

[63] Nakamura E, Kadomatsu K, Yuasa S, Muramatsu H, Mamiya T, Nabeshima T, et al. Disruption of the midkine gene (Mdk) resulted in altered expression of a calcium binding protein in the hippocampus of infant mice and their abnormal behaviour. Genes Cells 1998;3:811–22.

[64] Liedert A, Mattausch L, Rontgen V, Blakytny R, Vogele D, Pahl M, et al. Midkine-deficiency increases the anabolic response of cortical bone to mechanical loading. Bone 2011;48:945–51.

[65] Surjit M, Ganti KP, Mukherji A, Ye T, Hua G, Metzger D, et al. Widespread negative response elements mediate direct repression by agonist-liganded glucocorticoid receptor. Cell 2011;145:224–41.

BRIEF COMMUNICATION

Effect of dietary eugenol on xenobiotic metabolism and mediation of UDP-glucuronosyltransferase and cytochrome P450 1A1 expression in rat liver

Hidetomo Iwano[1], Wakako Ujita[1], Miyu Nishikawa[1], Satomi Ishii[2], Hiroki Inoue[3], and Hiroshi Yokota[1]

[1]Laboratory of Veterinary Biochemistry, Graduate School of Veterinary Medicine, [2]Department of Food Science, Faculty of Dairy Science, and [3]Laboratory of Environmental Biochemistry, Faculty of Environmental System, Rakuno Gakuen University, Ebetsu, Hokkaido, Japan

Abstract

Xenobiotic-metabolizing enzymes (XMEs) play an important role in the elimination and detoxification of xenobiotics and drugs. A variety of natural dietary agents are known to protect against cancer by inducing XME. To elucidate the molecular mechanism of XME induction, we examined the effect of dietary eugenol (4-allyl-1-hydroxy-2-methoxybenzene) on xenobiotic metabolism. In this study, rats were administered dietary eugenol for 4 weeks to investigate the various effects of UDP-glucuronosyltransferase (UGT) and cytochrome P450 (CYP) expression. In rats administered dietary eugenol, expression levels of hepatic CYP1A 1 were reduced to 40% than of the controls, while expression of hepatic UGT1A6, UGT1A7 and UGT2B1 increased to 2–3 times than observed in the controls. Hepatic protein levels of UGT1A6 and 2B1 were also elevated in the eugenol-treated rats. These results suggest that the natural compound eugenol improves the xenobiotic-metabolizing systems that suppress and induce the expression of CYP1A1 and UGT, respectively.

Introduction

In addition to affecting a wide variety of biological events, environmental contaminants from food and water affect can also cause a variety of diseases. While avoiding the ingestion of these contaminants may be difficult, our bodies are capable of metabolizing most of these substances using a variety of xenobiotic-metabolizing enzymes (XMEs). These XMEs can be classified into three main categories. The first category consists of phase I enzymes, mainly the cytochrome P450 (CYP) enzymes (Nebert & Gonzalez, 1987; Nelson et al., 1993). Most drugs are metabolized by CYP, either as part of detoxification or due to activation of a pathway for an inactive prodrug. The second category is referred to as phase II enzymes (Di Pietro et al., 2010; Mackenzie et al., 1997, 2003). These enzymes usually conjugate phase I products, but can also conjugate other intermediate compounds and intracellular substrates, such as steroids and bilirubin. The last category consists of drug transporters that are membrane-bound proteins involved in drug uptake or excretion (Barry et al., 2003; Hediger et al., 2004). Regulation of these XME is an important area of study because their gene expression is influenced by a wide variety of drugs and chemicals derived from food (Kong et al., 2001; Rushmore & Kong, 2002; Xu et al., 2005). Since disruption of the homeostatic control of XME can cause cancer and a wide variety of diseases, considerable research has been undertaken in the area of XME metabolism. Of the treatment methods currently available, stimulating the excretion of xenobiotic substances has been shown to restore the health of a subject (Aggarwal, 2008; Aggarwal & Shishodia, 2006). Eugenol (4-allyl-1-hydroxy-2-methoxybenzene) is weakly acidic, slightly soluble in water and soluble in organic solvent (Kamatou et al., 2012). It has been identified in several aromatic plants such as clove oil, cinnamon, basil and nutmeg as a food-flavoring agent; but thus far, the medical application of pure eugenol has been limited to the field of dentistry (Kamatou et al., 2012). In recent years, eugenol has been reported to have antioxidant and anti-inflammatory effects, and recent studies have shown that eugenol is capable of inhibiting melanoma cancer cell proliferation (Ghosh et al., 2005), inducing apoptosis in melanoma (Pisano et al., 2007) and human promyelocytic leukemia cells (HL-60) (Yoo et al., 2005), and is involved in a rat model of gastric carcinogenesis (Manikandan et al., 2010). These authors suggested that eugenol may be a candidate for putative chemopreventive and chemotherapeutic agents. Eugenol is a main component of clove oil and is also present in the essential oils of many other plant species, including cinnamon, basil and nutmeg (Aggarwal, 2008; Aggarwal & Shishodia, 2006). Thus, although eugenol is considered to be well suited for use as an anticancer drug, the mechanisms and molecules involved in the metabolism of this compound are currently unknown (Aggarwal, 2008; Aggarwal & Shishodia, 2006).

This study demonstrates that eugenol influenced the transcription of isoforms of the XMEs CYP (EC 1. 14. 14. 1) and UDP-glucuronosyltransferase (UGT) (EC 2. 4. 1. 17), suggesting that eugenol could potentially be used as an anticancer drug through maintaining the homeostasis of xenobiotic metabolism.

Correspondence: Hiroshi Yokota, Laboratory of Veterinary Biochemistry, Graduate School of Veterinary Medicine, Rakuno Gakuen University, 582 Bunkyodai-Midorimachi Ebetsu, Hokkaido 069-8501, Japan. Tel/Fax: +81-11-388-4743. E-mail: h-yokota@rakuno.ac.jp

RIGHTSLINK()